Study on the Damping Performance Characteristics Analysis of Shock Absorber of Vehicle by Considering Fluid Force

Choon-Tae Lee
Department of Mechanical and Intelligent Systems Engineering, Busan National University, 30 Changjeon-dong, Keumjeong-ku, Busan 609-735 Korea
Byung-Young Moon*
ILIC (Industrial Liaison Innovation Cluster), Pusan National Univeristy, 30 Jangjeon-dong, Geumjeong-gu, Busan 609-735, Korea

In this study, a new mathematical dynamic model of displacement sensitive shock absorber (DSSA) is proposed to predict the dynamic characteristics of automotive shock absorber. The performance of shock absorber is directly related to the vehicle behaviors and performance, both for handling and ride comfort. The proposed model of the DSSA has two modes of damping force (i.e. soft and hard) according to the position of piston. In this paper, the performance of the DSSA is analyzed by considering the transient zone for more exact dynamic characteristics. For the mathematical modeling of DSSA, flow continuity equations at the compression and rebound chamber are formulated. And the flow equations at the compression and rebound stroke are formulated, respectively. Also, the flow analysis at the reservoir chamber is carried out. Accordingly, the damping force of the shock absorber is determined by the forces acting on the both side of piston. The analytic result of damping force characteristics are compared with the experimental results to prove the effectiveness. Especially, the effects of displacement sensitive orifice area and the effects of displacement sensitive orifice length on the damping force are observed, respectively. The results reported herein will provide a better understanding of the shock absorber.

Key Words: Shock Absorber, Damping Force, Displacement Sensitive Orifice, Flow Continuity Equations, Stroke Dependent, Piston Valve, Mathematical Model

1. Introduction

The shock absorber is an important part of automotive which has an effects on ride characteristics such as ride comfort and driving safety. There have been several studies are carried out about the shock absorber. At first, Lang (1977) proposed a simple mathematical model of the passive shock absorber. After that many studies have been carried out to analyze the performance of shock absorber (Stefaan et al., 1997). Cherng et al.(1999) reported the noise effects of the shock absorber using acoustic index method. Koenraad (1994) proposed a mathematical model of mono-tube type gas charged shock absorber. Herr et al. (1999) proposed a mathematical model of twin tube type shock absorber. Simms et al.(2002) investigated the influence of damper properties on luxury vehicle dynamic behavior through the simulation and test. Liu et al.(2002) reported the characteristics of nonlinear dynamic response for the twin-tube hydraulic shock absorber. Nevertheless, there have been few studies carried out about DSSA.

* Corresponding Author,
E-mail : moonby@pusan.ac.kr
TEL : +82-51-510-3696; **FAX** : +82-51-514-3690
ILIC, Pusan National Univeristy, #11405 Engineering Bldg., 30 Jangjeon-dong, Geumjeong-gu, Busan 609-735, Korea. (Manuscript **Received** April 6, 2004; **Revised** December 21, 2004)

Recently, there is a study reported about the DSSA. However, it was insufficient to understand the dynamic characteristics of the DSSA completely (Park et al., 1997; Cho and So, 1999). Therefore, in this study a new mathematical and simulation model of the DSSA is proposed and analyzed, which considered the transient range of displacement sensitive orifice. A typical twin-tube type passive shock absorber of automotive is considered for the study of the operating principles of the DSSA. For the mathematical modeling of the DSSA, flow continuity equations at the compression and rebound chamber are formulated. And the flow equations at the compression stroke and at the rebound stroke are obtained, respectively. Also, the flow analysis at the reservoir chamber is carried out. Accordingly, the damping force of the shock absorber is determined by the forces acting on the both side of piston.

And the effects of displacement sensitive orifice area and soft zone length on the damping force of the DSSA are observed, respectively.

2. General Configuration and Operating Principles of DSSA

Basically the shock absorber consists of a piston which moves up and down in a fluid-filled cylinder. The cylinder is fastened to the axle or wheel suspension, and the piston is connected via the piston rod to the frame of the vehicle. As the piston is forced to move with respect to the cylinder, a pressure differential is developed across the piston, causing the fluid to flow through orifices and valves in the piston. The portion of the cylinder above the piston is known as the rebound chamber, and the portion of the cylinder below the piston is known as the compression chamber. And the volume which surrounds the cylinder is known as the reservoir chamber. The reservoir chamber is partially filled with fluid and partially filled with a gas phase, normally air. The fluid flow between the compression and reservoir chambers passes through the body valve assembly at the bottom of the compression chamber. Figure 1 illustrates the typical configuration of a DSSA. As can be observed in Fig. 1, the DSSA has an additional flow passages in the cylinder wall of a typical passive shock absorber. And this displacement sensitive orifices can be divided into three zone such as the soft, transient and hard zone. Here, the transient zone has tapered scheme to avoid abrupt changes of damping

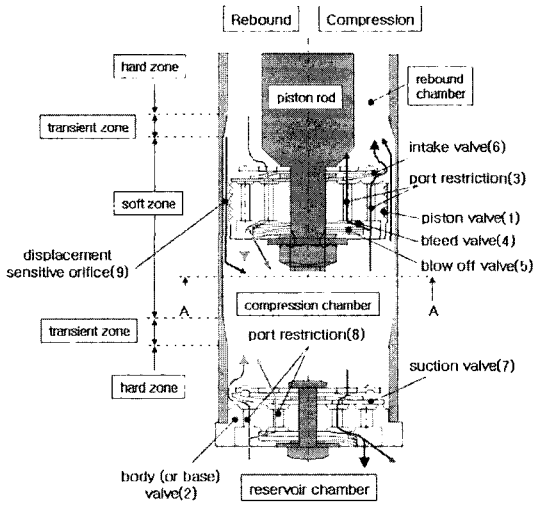

Fig. 1 Fluid flow pattern of the DSSA at compression and rebound stroke

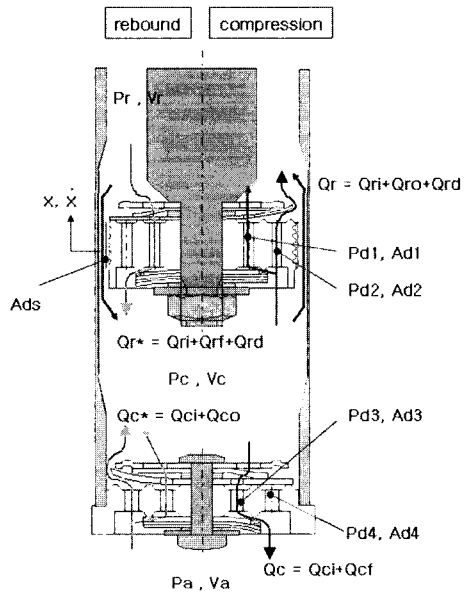

Fig. 2 Schematic diagram of the fluid flow and pressure at compression and rebound stroke

force. Each valves and corresponding chamber are described according to the fluid flow. Figure 2 illustrates the analytic model of the DSSA, which describes a fluid flow pattern according to piston movement.

The fluid flows at the compression stroke can be divided into two flows such as Q_r and Q_c. The first one, Q_r is a flow which flows from the compression chamber to rebound chamber through the piston valve (1) and the other one, Q_c is a flow which flows from compression chamber to reservoir chamber through body valve (2). Where the valve numbers are noted in Fig. 1. The flow Q_r which flows through the piston valve can be divided into three flows Q_{ri}, Q_{ro} and Q_{rd}. The flow Q_{rd} flows through bleed valve(4). The flow Q_{ro} flows through intake valve (6) and the flow Q_{rd} flows through displacement sensitive orifice (9) of piston valve, respectively. The flow Q_c which flows through the body valve (2) at the compression stroke can be divided into two flows Q_{ci}, Q_{cf}. The flow Q_{ci} flows through bleed valve and the flow Q_{cf} flows through a blow-off valve.

On the contrary, at the rebound stroke the fluid flows can be divided into two flows Q_r^*, Q_c^*. The first one Q_r^* is a flow which flows from the rebound chamber to compression chamber through piston valve (1) and the other one Q_c^* is a flow which flows from reservoir chamber to compression chamber through body valve (2). The flow Q_c^* which flows through body valve (2) can be divided into two flows Q_{ci}, Q_{co}. The flow Q_{ci} flows through bleed valve and the flow Q_{co} flows through suction valve (7). Also, the flow Q_r^* which flows through piston valve (1) can be divided into three flows Q_{ri}, Q_{rf} and Q_{rd}. The flow Q_{ri} flows through bleed valve (4), the flow Q_{rf} flows through blow off valve (5) and the flow Q_{rd} flows through displacement sensitive orifices, respectively.

3. Mathematical Modeling of the DSSA

3.1 Flow continuity equations at the compression and rebound chamber

The flow continuity equations of the compression chamber at the rebound stroke, as described in Fig. 3, can be expressed as follows;

$$\frac{V_c}{K}\frac{\partial P_c}{\partial t}=-A_p\dot{x}+(Q_r^*+Q_c^*) \tag{1}$$

The flow continuity equation of the compression chamber at the compression stroke, can be expressed as follows;

$$\frac{V_c}{K}\frac{\partial P_c}{\partial t}=A_p\dot{x}-(Q_r+Q_c) \tag{2}$$

where K is a bulk modulus of elasticity of working fluid. V_c is a volume of compression chamber. P_c is a pressure of compression chamber. A_p is an area of piston. $\dot{x}$ is a velocity of piston.

Similar way, the flow continuity equation of the rebound chamber at the rebound stroke can be expressed as follows;

$$\frac{V_r}{K}\frac{\partial P_r}{\partial t}=(A_p-A_{rod})\dot{x}-Q_r^* \tag{3}$$

The flow continuity equation of the rebound chamber at the compression stroke can be expressed as follows;

$$\frac{V_r}{K}\frac{\partial P_r}{\partial t}=-(A_p-A_{rod})\dot{x}+Q_r \tag{4}$$

where V_r is a volume of rebound chamber. P_r is a pressure of rebound chamber. A_{rod} is an area of piston rod.

3.2 Flow equations at the compression stroke

The flow rate of the piston valve Q_r, which flows between the rebound and compression chambers at the compression stroke can be expressed as follows;

$$Q_r=Q_{ri}+Q_{ro}+Q_{rd} \tag{5}$$

Here, each flow rates can be obtained as follows;

$$\begin{aligned}Q_{ri}&=C_dA_{pb}\sqrt{\frac{2}{\rho}(P_c-P_{d1})}\\&=C_dA_{d1}\sqrt{\frac{2}{\rho}(P_{d1}-P_r)}\end{aligned} \tag{6}$$

$$Q_{ro}=C_dA_{d2}\sqrt{\frac{2}{\rho}(P_c-P_{d2})}=Q_{in}\frac{P_{d2}-P_{icr}}{P_{im}-P_{icr}} \tag{7}$$

Here, when $P_{d2}<P_{icr}$, P_{ro} becomes zero.

$$Q_{rd}=C_dA_{ds}(x)\sqrt{\frac{2}{\rho}(P_c-P_r)} \tag{8}$$

$$A_{ds}(x)=\begin{cases} w\left\{\dfrac{h}{z_2}(x+z_1)+h\right\} & (z_1<x\leq(z_1+z_2)) \\ wh & (-z_1<x\leq z_1) \\ w\left\{-\dfrac{h}{z_2}(x-z_1)+h\right\} & (-(z_1+z_2)<x\leq -z_1) \end{cases} \tag{9}$$

where C_d is a coefficient of discharge. A_{pb} is a bleed valve(4) orifice area of piston valve. A_{d1}, A_{d2} are areas of piston valve port restriction (3). P_{d1} and P_{d2} are pressures at the piston valve port restriction (3). Q_{im} is a maximum flow rate of the intake valve (6). P_{icr} is a cracking pressure of intake valve (6). P_{im} is a pressure of intake valve (6) at the maximum flow rate Q_{im}. Figure 3 shows detailed configuration of displacement sensitive orifice. A_{ds} is an area of displacement sensitive orifice, as shown in Fig. 3.

The flow rate Q_{rd} becomes zero when the displacement of piston detach from displacement sensitive orifice. And the flow rate of the body valve Q_c, which flows between the reservoir and compression chambers at the compression stroke can be expressed as follows;

$$Q_c=C_dA_{d3}\sqrt{\frac{2}{\rho}(P_c-P_{d3})}=Q_{ci}+Q_{cf} \tag{10}$$

Each flow rates of Eq. (10) can be obtained as follows;

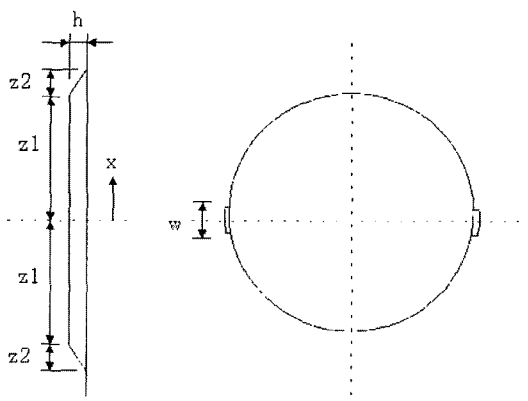

Fig. 3 Detailed configuration of displacement sensitive orifice

$$Q_{ci}=C_dA_{bb}\sqrt{\frac{2}{\rho}(P_{d3}-P_a)} \tag{11}$$

$$Q_{cf}=Q_{bm}\frac{(P_{d3}-P_{bcr})}{(P_{bm}-P_{bcr})} \tag{12}$$

Here, when $P_{d3}<P_{bcr}$, Q_{cf} becomes zero. Where A_{bb} is a bleed valve orifice area of the body valve (2). A_{d3} is a port restriction area (8) of body valve. P_{d3} is a pressure at the port restriction of the body valve (2). P_a is a pressure of reservoir chamber. Q_{bm} is a maximum flow rate of the blow off valve at the body valve. P_{bcr} is a cracking pressure of the blow off valve at the body valve. P_{bm} is a pressure of the blow off valve at the maximum flow rate at the body valve.

3.3 Flow equations at the rebound stroke

The flow rate of the piston valve Q_r^*, which flows between rebound and compression chambers at the rebound stroke can be expressed as follows;

$$Q_r^*=Q_{ri}+Q_{rf}+Q_{rd} \tag{13}$$

$$Q_{ri}=C_dA_{pb}\sqrt{\frac{2}{\rho}(P_{d1}-P_c)} \tag{14}$$

$$Q_{rf}=Q_{pm}\frac{(P_{d1}-P_{pcr})}{(P_{pm}-P_{pcr})} \tag{15}$$

Here, when $P_{d1}<P_{pcr}$, Q_{rf} becomes zero.

$$Q_{rd}=C_dA_{ds}(x)\sqrt{\frac{2}{\rho}(P_r-P_c)} \tag{16}$$

where Q_{pm} is a maximum flow rate of blow off valve (5) at the piston valve. P_{pcr} is a cracking pressure of the blow off valve at the piston valve. P_{pm} is a pressure of the blow off valve at the maximum flow rate of the piston valve. Q_{rd} becomes zero when the displacement of piston detach from displacement sensitive zone. And the flow rate of body valve Q_c^*, which flows between the reservoir and compression chambers at the rebound stroke can be expressed as follows;

$$Q_c^*=Q_{ci}+Q_{co} \tag{17}$$

$$Q_{ci}=C_dA_{bb}\sqrt{\frac{2}{\rho}(P_a-P_{d3})} \\ =C_dA_{d3}\sqrt{\frac{2}{\rho}(P_{d3}-P_c)} \quad (18)$$

$$Q_{co}=C_dA_{d4}\sqrt{\frac{2}{\rho}(P_a-P_{d4})} \\ =Q_{sm}\frac{(P_{d4}-P_{scr})}{(P_{sm}-P_{scr})} \quad (19)$$

Here, when $P_{d4}<P_{scr}$, Q_{cf} becomes zero. Where A_{d4} is a port restriction (8) area of the body valve. P_{d4} is a pressure at the body valve port restriction (8). Q_{sm} is a maximum flow rate of suction valve (7). P_{scr} is a cracking pressure of suction valve. P_{sm} is a pressure at the maximum flow rate of suction valve.

3.4 Flow analysis at the reservoir chamber

Because the piston rod passes through the rebound chamber, and is connected to the rebound side of the piston, the area of the rebound side is less than the area of the compression side of the piston. Accordingly, as the piston moves, the combined volume of the compression and rebound chambers changes by an amount equivalent to the inserted, or withdrawn piston rod volume. The amount of fluid equivalent to the inserted, or withdrawn, piston rod volume must be transferred to, or from, the reservoir chamber which normally surrounds the cylinder. Air pressure of the reservoir chamber can be expressed as an ideal gas equation as follows;

$$P_aV_a=m_aRT \quad (20)$$

where P_a is an air pressure of the reservoir chamber. V_a is an air volume of reservoir chamber. m_a is an air mass of reservoir chamber. R is a gas constant. T is an temperature of air in the reservoir chamber.

Generally, the mass of air is assumed constant because the chamber is sealed. And the temperature T of the reservoir chamber assumed constant to simplify the analysis. Accordingly, the air of the reservoir chamber can be expressed as ideal gas equation as follows;

$$P_aV_a=const \quad (21)$$

The time variation V_a of air volume of reservoir chamber can be expressed as follows.

$$V_a(t)=V_{ao}-\int Q_cdt \quad (22)$$

Where, V_{ao} is an initial air volume of the reservoir chamber. Therefore, the air pressure variation of the reservoir chamber can be obtained from the Eqs. (20) and (22) as follows;

$$P_a=\frac{m_aRT}{V_{ao}-\int Q_cdt} \quad (23)$$

3.5 Damping force of the shock absorber

The damping force of the shock absorber is determined by the forces acting on the both side of piston. Figure 4 shows free body diagram of the piston.

By considering the forces acting on the piston, the damping force can be obtained as follows;

$$F_{damping}=P_rA_r-P_cA_p\pm F_{friction} \quad (24)$$

$$A_r=A_p-A_{rod} \quad (25)$$

Where $F_{damping}$ is a damping force. $F_{friction}$ is the friction forces, which acting on piston rod. Here, the friction forces are another factor that determines damping force. But, in this study, the friction forces are ignored to simplify the analysis.

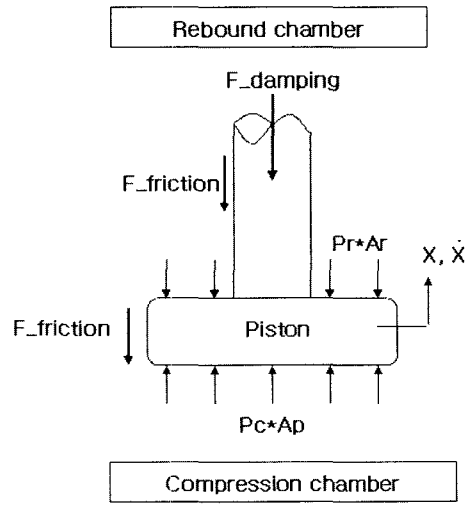

Fig. 4 Free body diagram of the piston

4. Results of the Analysis and Discussion

4.1 Analysis results

A simulation model of the DSSA is shown in Fig. 5. The simulation model is structured by using the AMESIM ver4.0 of Imagine Co.. The input of excitation in simulation model is composed of displacement-velocity transformer, which transforms a input displacement into the velocity. Reservoir chamber is modeled with the real air properties by using pneumatic module of the AMESIM. The displacement sensitive orifice is modeled with function block $f(x)$ and variable hydraulic restrictor. And the function block $f(x)$ calculated the opening area of variable hydraulic restrictor by using the piston stoke. The main physical properties of the simulation model are listed in Table 1.

Figure 6 shows simulation results of stroke-damping force diagram for the excitation velocity of 0.1, 0.2, 0.3, 0.6 and 1.0 m/sec, respectively. The damping force changes from soft to hard mode due to the displacement sensitive characteristics around the stroke at ±20 mm, as shown in Fig. 6. Especially, as can be seen in Fig. 6, the damping force changes smoothly around the transient zone. It is well illustrate the function of transient zone which prevent abrupt changes of damping force. To verify the reliability of simulation results of the proposed model, experimental results are presented in Fig. 7. As can be observed in Fig. 7, the experimental result shows very similar tendency with the result of this study.

Figure 8 shows the variations of the damping force characteristic according to the variations of the displacement sensitive orifice area. The

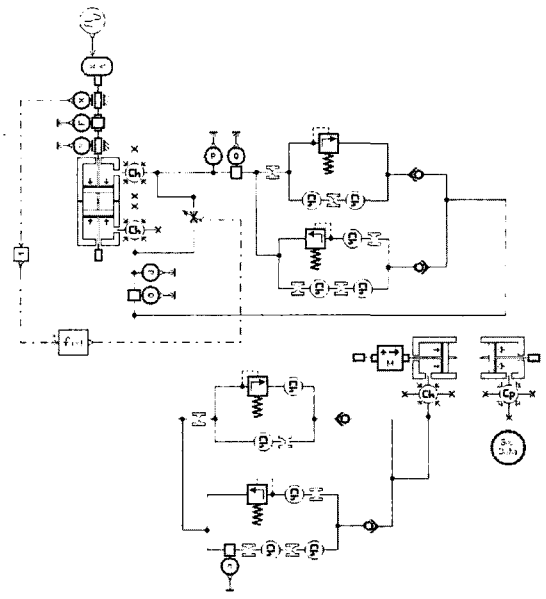

Fig. 5 Simulation model of the DSSA

Table 1 Simulation parameters

piston diameter	30 mm
piston rod diameter	16 mm
reservoir chamber inner diameter	32 mm
reservoir chamber outer diameter	42 mm
initial oil height in reservoir chamber	100 mm
sinusoid displacement input	±40 mm 0~4.0 Hz
initial rebound chamber volume	63 cm^3
initial compression chamber volume	88.4 cm^3
initial reservoir chamber volume	65.9 cm^3
perfect gas constant	0.287 J/g/K
absolute viscosity of gas	1.82e-5 Ns/m^2
hydraulic oil density	850 kg/m^3
hydraulic oil bulk modulus	1,700 MPa
hydraulic oil kinematic viscosity	5e-5 m^2/s
hydraulic oil temperature	40℃

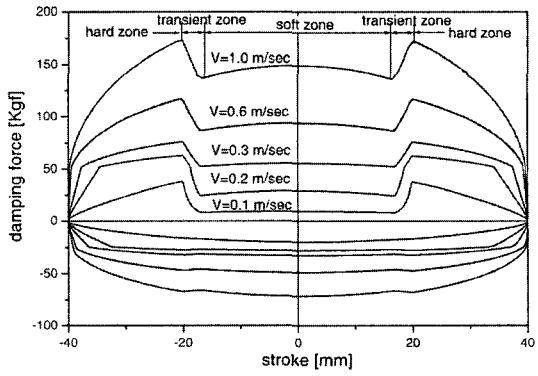

Fig. 6 Analytical result of the DSSA in damping force diagram

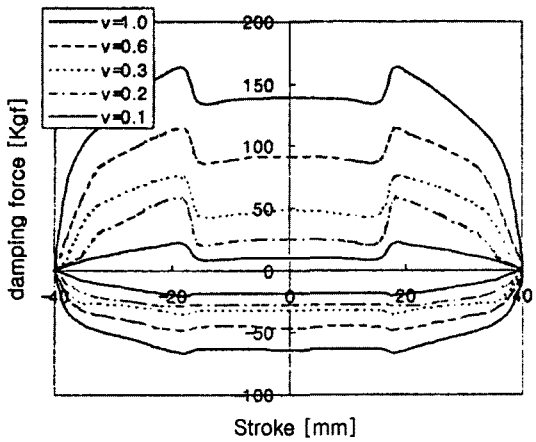

Fig. 7 Experimental result of the DSSA damping force diagram

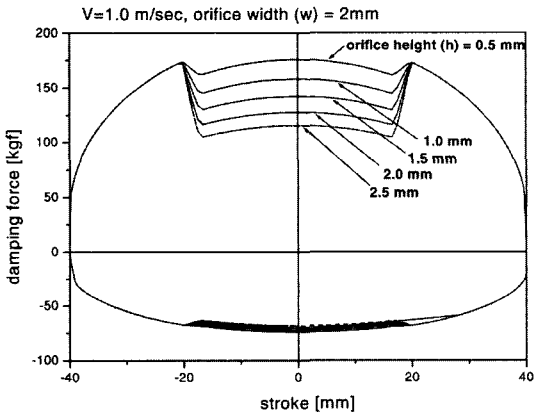

Fig. 8 Effects of displacement sensitive orifice area on the damping force diagram of the DSSA

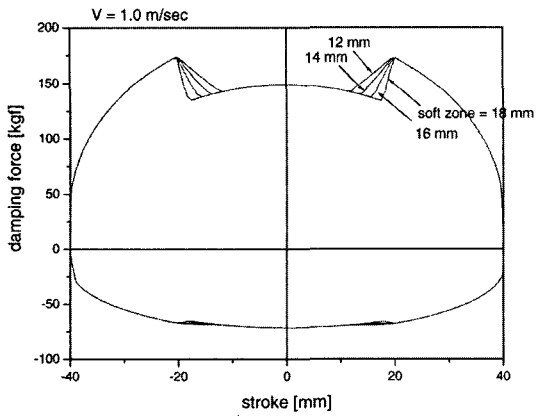

Fig. 9 Effects of the soft zone length of the displacement sensitive orifice on the damping force diagram of the DSSA

excitation velocity is 1 m/sec and the width of orifice is 2 mm. Fig. 8 shows the characteristics of stroke-damping force when the height of displacement sensitive orifice is varied into 0.5, 1.0, 1.5, 2.0, 2.5 mm, respectively. As shown in Fig. 8, it can be observed that the increasing rate of

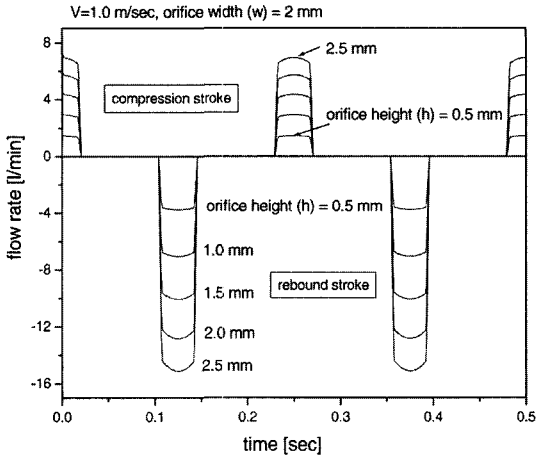

Fig. 10 Flow rate through displacement sensitive orifice according to displacement sensitive orifice area

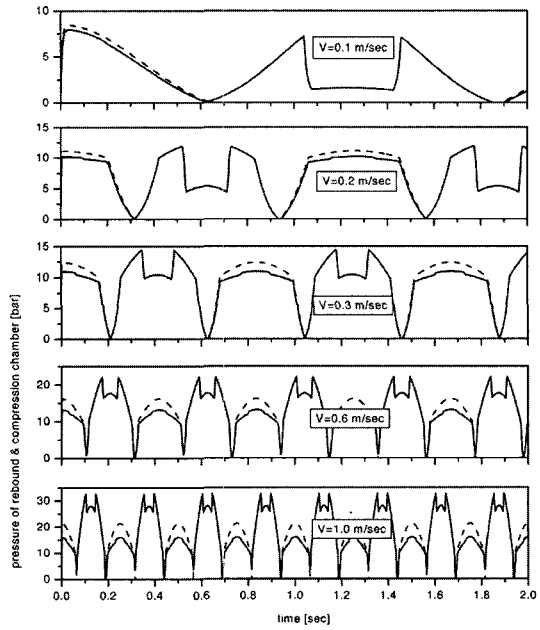

Fig. 11 The variation of the pressure of rebound and compression chamber according to the change of the excitation velocity

damping force increase gradually according to the decrease of orifice height.

Figure 9 shows the variations of damping force characteristic according to the soft zone length variations of displacement sensitive orifice. The excitation velocity is 1 m/sec. Figure 9 shows the characteristics of stroke-damping force when the soft zone length is varied into 12, 14, 16, 18 mm, respectively. As shown in figure, it can be observed that the damping force varies in transient range with the variation of the orifice length. Nevertheless, there is no change of the damping force in soft zone.

Figure 10 shows variations of the flow rate through displacement sensitive orifice according to the changes of displacement sensitive orifice area. Figure 11 shows variations of the pressure of the rebound and compression chamber according to the changes of excitation velocity. In the figure, solid line stands for the pressure variation of the rebound chamber and dash line stands for the pressure variation of compression chamber, respectively. In the figure, excitation velocity 1.0 m/sec which is corresponds to the 4 Hz excitation frequency. And the results shows well the characteristics of pressure variation according to the excitation velocity both in rebound and compression chambers.

5. Conclusions

In this study, a new mathematical nonlinear dynamic model is proposed to predict the performance of the DSSA. A typical twin-tube type passive shock absorber of automotive is considered for the study of operating principles of the DSSA. For the mathematical modeling of the DSSA, a flow continuity equations at the compression and the rebound chamber are formulated. And the flow equations at the compression and the rebound stroke are formulated, respectively. Also, the flow analysis at the reservoir chamber is carried out by considering the real property of the air and working fluid. Accordingly, the damping force of the shock absorber is determined by the forces acting on the both side of piston.

The analytical results of the DSSA in stroke-damping force are compared with the experimental results to prove the effectiveness of the proposed simulation model. And the effects of displacement sensitive orifice area and soft zone length on the damping force of the DSSA are observed, respectively. Flow rate through displacement sensitive orifice according to displacement sensitive orifice area shows the efficiency of the proposed method. Pressure of the rebound and compression chamber are analyzed reasonably according to the proposed method. The results reported herein will provide a better understanding of the shock absorber. Moreover, it is believed that those properties of the results can be utilized in the dynamic design of the automotive system.

Acknowledgment

This work was supported by grant No. R08-2003-000-11075-0 from the Basic Research Program of the Korea Science & Engineering Foundation and the authors wishes to thank for this support.

References

Adrian Simms, David Crolla, 2002, "The Influence of Damper Properties on Vehicle Dynamic Behavior," *SAE 2002-01-0319*, pp. 79~86.

Herr, F., Malin, T., Lane, J. and Roth, S., 1999, "A Shock Absorber Model Using CFD Analysis and Easy 5," in: *Proceedings of the 1999 SAE International Congress and Exposition*, 1999-01-1322.

Jaewoo Park, Dongwoo Joo and Youngho Kim, 1997, "A Study on the Stroke Sensitive Shock Absorber," *Journal of Korean Society of Precision Engineering*, 14, pp. 11~16.

John G. Cherng, Tone Ge, John Pipis and Richard Gazala, 1999, "Characterization of Air-Borne Noise of Shock Absorber by Using Acoustics Index Method," in: *Proceedings of the 1999 SAE International Congress and Exposition*, 1999-01-1838.

Koenraad Reybrouck, 1994, "A Nonlinear Parametric Model of an Automotive Shock Absorber," *SAE 940869*, pp. 79~86.

Kyungil Cho and Sanggyun So, 1999, "A Study of the New Typed Stroke Dependent Damper," *J of KSAE*, Vol. 7, No. 3, pp. 294~300.

Lang Harold Harvey, 1977, "A Study of the Characteristics of Automotive Hydraulic Dampers at High Stroking Frequencies," *Ph. D. Thesis, Department of Mechanical Engineering*, University of Michigan, U.S.A..

Liu, Y., Zhang, J., Yu, F. and Li, H., 2002, "Test and Simulation of Nonlinear Dynamic Response for the Twin-tube Hydraulic Shock Absorber," *SAE 2002-01-0320*, pp. 91~98.

Stefaan W. Duym, Randy Stiens, Gino V. Baron and Koenraad G. Reybrouck, 1997, "Physical Modeling of the Hysteretic Behavior of Automotive Shock Absorbers," *SAE (Society of Automotive Engineers) 970101*, pp. 125~137.